Inorg. Chem. **2005**, *44*, 2031–2038

Synthesis, Characterization, and Structures of $Mn(DMHP)_3 \cdot 12H_2O$ and $Mn(DMHP)_2Cl \cdot 0.5H_2O$

Wen-Yuan Hsieh and Shuang Liu*

Department of Industrial and Physical Pharmacy, School of Pharmacy, Purdue University, 575 Stadium Mall Drive, West Lafayette, Indiana 47907

Received July 15, 2004

This report describes the synthesis, characterization, and X-ray crystal structures of two Mn(III) complexes, $Mn(DMHP)_3 \cdot 12H_2O$ and $Mn(DMHP)_2Cl \cdot 0.5H_2O$ (DMHP = 1,2-dimethyl-3-hydroxy-4-pyridinone). $Mn(DMHP)_2Cl$ was prepared from the reaction of Mn(II) chloride with 2 equiv of DMHP under reflux in the presence of triethylamine. $Mn(DMHP)_3$ was obtained by reacting Mn(II) acetate with 3 equiv of DMHP in the presence of sodium acetate. $Mn(DMHP)_3$ could also be prepared by reacting $Mn(OAc)_3 \cdot 2H_2O$ with 3 equiv of DMHP in the presence of triethylamine. Both Mn(III) complexes have been characterized by elemental analysis, infrared spectroscopy, electronic paramagnetic resonance, electrospray ionization spectroscopy, electrochemical method, and X-ray crystallography. The X-ray crystal structure of $Mn(DMHP)_2Cl \cdot 0.5H_2O$ revealed a rare example of five-coordinated Mn(III) complexes with two bidentate ligands and a square pyramidal coordination geometry. Surprisingly, the average Mn–O (hydroxy) bond distance in $Mn(DMHP)_2Cl \cdot 0.5H_2O$ is ~0.025 Å longer than that of the average Mn–O (carbonyl) bond, suggesting an extensive delocalization of electrons in the two pyridinone rings. The structure of $Mn(DMHP)_3 \cdot 12H_2O$, a rare example of six-coordinate high-spin Mn(III) complexes without Jahn–Teller distortion, is isostructural to $M(DMHP)_3 \cdot 12H_2O$ (M = Al, Ga, Fe, and In). The electrochemical data for $Mn(DMHP)_3$ suggests that the Mn(III) oxidation state is highly stabilized by three DMHP ligands. DMHP has the potential as a chelator for the removal of excess intracellular Mn and the treatment of chronic Mn toxicity.

Introduction

Manganese (Mn) is an essential trace element for humans. The human body contains 10−20 mg of Mn, most of which is found in the liver, bones, brain, and kidneys.[1] Mn is a cofactor for a number of enzymes, including arginase, cholinesterase, phosphoglucomutase, pyruvate carboxylase, mitochondrial superoxide dismutase, and several phosphates, peptidases, and glycosyltransferases. Mn metabolism is similar to that of iron and is absorbed in the small intestine. While the absorption process is slow, the total absorption rate is exceptionally high (~40%). Excess Mn is excreted via bile and pancreatic secretion. Only a small amount is excreted in the urine.

Excess Mn interferes with the absorption of dietary iron. The increased Mn intake also impairs the activity of copper metallo-enzymes. Mn overload is generally due to industrial pollution. Workers in the Mn processing industry are most at risk.[2] Well water rich in Mn can also be the cause of excessive Mn intake.[3] Mn poisoning has been found among workers in the mining, welding, and battery manufacturing industries.[2] A significant increase in the Mn concentration was found in patients with severe hepatitis and posthepatic cirrhosis and in patients suffering heart attacks.[4−6] The prolonged exposure to high levels of Mn by inhalation in humans results primarily in central nerve system effects.

Chronic Mn intoxication in humans causes permanent neurodegenerative damage in the nigrostriatal region, resulting in a syndrome similar to Parkinson's disease.[7,8] While

* Author to whom correspondence should be addressed. Phone: 765-494-0236. Fax: 765-496-3367. E-mail: lius@pharmacy.purdue.edu.

(1) HaMai, D.; Bondy, S. C.; Campbell, A.; Becaria, A. *Curr. Top. Med. Chem.* **2001**, *1*, 541.
(2) Wang, J. D.; Huang, C. C.; Hwang, Y. H.; Chiang, J. R.; Lin, J. M.; Chen, J. S. *Br. J. Ind. Med.* **1989**, *46*, 856.
(3) Kilburn, C. J. *Neurotoxicology* **1987**, *8*, 421.
(4) Alves, G.; Thiebot, J.; Tracqui, A.; Delangre, T.; Guedon, C.; Lerebours, E. *JPEN* **1997**, *21*, 41.
(5) Krieger, D.; Krieger, S.; Jansen, O.; Gass, P.; Theilmann, L.; Lihctnecker, H. *Lancet* **1995**, *346*, 270.
(6) Pomier-Layrargues, G.; Spahr, L.; Butterworth, R. F. *Lancet* **1995**, *345*, 735.
(7) Dobson, A. W.; Erikson, K. M.; Aschner, M. *Ann. N.Y. Acad. Sci.* **2004**, *1012*, 115.

10.1021/ic0490627 CCC: $30.25
Published on Web 02/22/2005

the etiology of idiopathic Parkinson's disease (IPD) remains unclear, high levels of total iron, decreased ferritin, and oxidative stress have been observed in substantia nigra of IPD patients.[9−13] A recent study has demonstrated that the serum Fe concentration is significantly reduced in IPD patients compared with controls, suggesting a compartment shift in Fe from blood to tissues, including the brain.[14] It has been suggested that the Mn-induced neurotoxicities might be associated with its interaction with Fe-containing enzymes at systemic and cellular levels[15−17] and the increased oxidative stress.[18,19] Following Mn exposure, there is a predominant influx of Fe from the blood into the cerebrospinal liquid (CSF) and from the extracellular matrix to intracellular space.[16,17] It has been reported that Mn(III) has higher cytotoxicity than Mn(II).[20] The neurodegeneration induced by Mn is most likely caused by the increased iron oxidation kinetics accelerated by Mn(III).[21] Thus, there is an unmet medical need for chelators, which are able to remove excess Mn(III) and Fe(III) from the intracellular matrix. Since both Mn and Fe are present in excess in the intracellular matrix, the Mn(III)/Fe(III) selectivity of a potential chelator is not necessary.

Mn resembles Fe in several ways: having similar ionic radii, carrying both +2 and +3 oxidation states under physiological conditions, and processing a similar affinity for the carrier protein, transferrin.[21] Because of these similarities, chelators with high affinity and selectivity toward Fe(III) should be useful for the removal of excess intracellular Mn(III). Figure 1 shows selected iron chelators. Desferrioxamine-B (DFO) is the most widely used ion chelator for the last 30 years, but DFO is orally inactive. DMHP (1,2-dimethyl-3-hydroxy-4-pyridinone) is the only orally active iron chelator currently available in clinic (marketed by Apotex, Inc., Toronto, Canada, as Ferripox) for the treatment of iron overload in thalassemia patients.[22−26] For the last two decades, N-substituted 3-hydroxy-4-pyridinones (3,4-HPs)

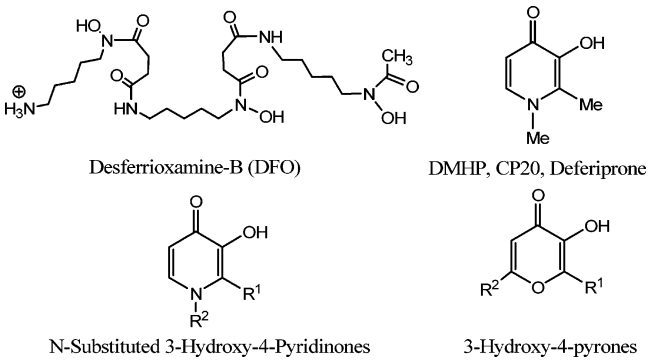

Figure 1. Examples of iron chelators. DMHP is the only orally active iron chelator currently in clinical use (marketed by Apotex, Inc., Toronto, Canada, as Ferripox) for the treatment of iron overload in β-thalassemia patients.

have been studied for their coordination chemistry with metal ions, such as Al(III), Ga(III), In(III), and Fe(III).[27−34] However, very little information is available about Mn(III) complexes of DMHP and 3,4-HPs.

We are interested in DMHP for its potential as a chelator in the treatment of chronic Mn toxicity. To understand the fundamental coordination chemistry of Mn(III) with DMHP and 3,4-HPs, we prepared two Mn(III) complexes, Mn(DMHP)$_3$ and Mn(DMHP)$_2$Cl. The purpose of this study is to demonstrate the structural similarity between tris-DMHP complexes of Fe(III) and Mn(III). In this report we present synthesis, characterization, and X-ray crystal structures of Mn(DMHP)$_3$·12H$_2$O and Mn(DMHP)$_2$Cl·0.5H$_2$O.

Experimental Section

Materials and Methods. Chemicals were purchased from Sigma Aldrich (St. Louis, MO), and were used as received. IR spectra were recorded on a Perkin-Elmer spectrum One FT-IR spectrometer. Mass spectral data were collected using both positive and negative modes on a Finnigan LCQ classic mass spectrometer, School of Pharmacy, Purdue University. Elemental analysis was performed by Dr. H. Daniel Lee using a Perkin-Elmer Series III analyzer, Department of Chemistry, Purdue University. X-Band continuous-wave (CW) perpendicular-mode electron paramagnetic resonance (EPR) spectra were collected on a Bruker EMX200E spectrometer, Department of Chemistry, University of Michigan. EPR spectra were collected at 120 K using a Varian liquid nitrogen continuous-flow cryostat. Mn complexes were dissolved in acetonitrile to form 2 mM solutions; 10% of toluene was added as glassing agent. The samples were frozen in liquid N_2 before measurement. Room-temperature UV−vis spectra were taken in acetonitrile from 250 to 800 nm and were recorded on a Beckman DU-640 UV−vis spectrometer.

(8) HaMai, D.; Bondy, S. *Neurochem. Int.* **2004**, *44*, 223.
(9) Dexter, D. T.; Carayon, A.; Javoy-Agid, F.; Agid, Y.; Wells, F. R.; Daniel. S. E.; Lees, A. J.; Jenner, P.; Marsden, C. D. *Brain* **1991**, *114*, 1953.
(10) Jenner, P.; Schapira, A. H.; Marsden, C. D. *Neurology* **1992**, *42*, 2241.
(11) Sofic, E.; Paulus, W.; Jellinger, K.; Riederer, P.; Youdim, M. B. H. *J. Neurochem.* **1991**, *56*, 978.
(12) Ye, F. Q.; Allen, P. S., Martin, W. R. *Mov. Dis.* **1996**, *11*, 243.
(13) Youdim, M. B.; Ben-Shachar, D.; Riederer, P. *Mov. Dis.* **1993**, *8*, 255.
(14) Logroscino, G.; Marder, K.; Graziano, J. H.; Freyer, G.; Slavkovich, V.; Lolacono, N.; Cote, L.; Mayeux, R. *Neurology* **1997**, *49*, 714.
(15) Zheng, W.; Ren, S.; Graziano, J. H. *Brain Res.* **1998**, *799*, 334.
(16) Zheng, W.; Zhao, Q.; Slavkovich, V. Aschner, M.; Graziano, J. H. *Brain Res.* **1999**, *833*, 125.
(17) Zheng, W.; Zhao, Q. *Brain Res.* **2001**, *897*, 175.
(18) HaMai, D.; Bondy, S. *Ann. N.Y. Acad. Sci.* **2004**, *1012*, 129.
(19) HaMai, D.; Campbell, A.; Bondy, S. *Free Radical Biol. Med.* **2001**, *31*, 763.
(20) Chen, J. Y.; Tsao, G. C.; Zhao, Q.; Zheng, W. *Toxicol. Appl. Pharmacol.* **2001**, *175*, 160.
(21) Aschner, M.; Vrana, K. E.; Zheng, W. *Neurotoxicology* **1999**, *20*, 173.
(22) Liu, Z. D.; Hider, R. C. *Med. Res. Rev.* **2002**, *22*, 26; references therein.
(23) Liu, Z. D.; Hider, R. C. *Coord. Chem. Rev.* **2002**, *232*, 151 and references therein.
(24) Richardson, D. R. *J. Lab. Clin. Med.* **2001**, *137*, 324.
(25) Taher, A.; Sheikh-Taha, M.; Koussa, S.; Inati, A.; Neeman, R.; Mourad, F. *Eur. J. Haematol.* **2001**, *67*, 30.
(26) Cohen, A. R.; Galanello, R.; Piga, A.; DiPalma, A.; Vullo, C.; Tricta, F. *Brit. J. Haematol.* **2000**, *108*, 305.
(27) Nelson, W. O.; Rettig, S. J.; Orvig, C. *J. Am. Chem. Soc.* **1987**, *109*, 4121.
(28) Nelson, W. O.; Karpishin, T. B.; Rettig, S. J.; Orvig, C. *Inorg. Chem.* **1988**, *27*, 1045.
(29) Nelson, W. O.; Rettig, S. J.; Orvig, C. *Inorg. Chem.* **1989**, *28*, 3153.
(30) Matsuba, C. A.; Nelson, W. O.; Rettig, S. J.; Orvig, C. *Inorg. Chem.* **1988**, *27*, 3935.
(31) Clevette, D. J.; Nelson, W. O.; Nordin, A.; Orvig, C.; Sjöberg, S. *Inorg. Chem.* **1989**, *28*, 2079.
(32) Clevette, D. J.; Lyster, D. M.; Nelson, W. O.; Rihela, T.; Webb, G. A.; Orvig, C. *Inorg. Chem.* **1990**, *29*, 667.
(33) Clarke, E. T.; Martell, A. E.; Reibenspies, J. *Inorg. Chim. Acta* **1992**, *196*, 177.
(34) Xiao, G. Y.; van der Helm, D.; Hider, R. C.; Dobbin, P. S. *J. Chem. Soc., Dalton Trans.* **1992**, 3265.

Synthesis of Mn(DMHP)$_2$Cl. To a solution of DMHP (0.280 g, 2 mmol) and triethylamine (280 μL, 2 mmol) in 40 mL of acetonitrile was added $MnCl_2$ (0.126 g, 1 mmol). The resulting mixture was refluxed for 6 h, during which time the solution became dark green. After the mixture was cooled to room temperature, the volume of solvent was reduced to ~5 mL on a rotary evaporator. Cold diethyl ether (100 mL) was added to the solution to form a greenish-brown precipitate. The solid was filtered, washed with diethyl ether, and was then dried under vacuum overnight before being submitted for elemental analysis. The yield of the product was 0.315 g (83.8%). The greenish-brown solid was redissolved in a mixture of acetonitrile and ethanol (50%:50% = v:v). Slow evaporation of solvents afforded crystals for X-ray crystallographic analysis. IR (KBr, cm^{-1}): 1456, 1501, 1547 and 1605 (s, $\upsilon_{C=O}$ and υ_{ring}), and 3434 (bs, υ_{O-H}). Mass spectrometry (MS) (electrospray ionization (ESI), positive mode): $m/z = 331.13$ for $[C_{14}H_{16}MnN_2O_4]^+$. Anal. Calcd for Mn(DMHP)$_2$Cl·0.25H$_2$O: C, 45.34; H, 4.45; N, 7.56. Found: C, 45.27; H, 4.42; N, 7.57.

Synthesis of Mn(DMHP)$_3$. To a solution of DMHP (0.420 g, 3 mmol) and sodium acetate trihydrate (0.137 g, 1 mmol) in 50 mL of methanol was added $Mn(OAc)_2$·4H$_2$O (0.245 g, 1 mmol). The solution quickly turned dark green. The mixture was heated to reflux for 4 h. After the mixture was cooled to room temperature, a dark-green solid was formed. The solid was filtered, washed with diethyl ether, and dried under vacuum overnight before being submitted for elemental analysis. The yield was 0.435 g (84.6%). The same Mn(III) complex can also be prepared by reacting $Mn(OAc)_3$·2H$_2$O with 3 equiv of DMHP in the presence of triethylamine. Recrystallization from water afforded dark-green crystals suitable for X-ray crystallographic analysis. IR (KBr, cm^{-1}): 1455, 1502, 1548 and 1606 (s, $\upsilon_{C=O}$ and υ_{ring}), and 3435 (bs, υ_{O-H}). MS (ESI, positive mode): $m/z = 468.82$ for $[C_{21}H_{24}MnN_3O_6]^+$. Anal. Cacld for Mn(DMHP)$_3$·2.5H$_2$O: C, 49.03; H, 5.64; N, 8.17. Found: C, 49.05; H, 5.74; N, 8.08.

Electrochemistry. Cyclic voltammograms of Mn(III) complexes were recorded on a Bioanalytical System BAS-100A electrochemical analyzer. A standard three-electrode cell was used with a polished glassy-carbon working electrode, a Pt wire auxiliary electrode, an Ag/AgCl in 3 M NaCl as the reference electrode, and 0.1 M tetrabutylammonium hexafluorophosphate ($TBAPF_6$) as the supporting electrolyte. Before measurements, the sample solution was purged with extra pure N_2 gas to remove the dissolved oxygen and a continuous N_2 gas stream was blanketed over the solution during the experiment. The room-temperature bulk electrolysis was performed using a Pt gauze as the working electrode, a Pt wire as the auxiliary electrode, and a Ag wire as the reference electrode in acetonitrile with 0.1 M $TBAPF_6$ as the supporting electrolyte.

X-ray Crystallographic Analysis. Crystallographic data for Mn(DMHP)$_3$·12H$_2$O and Mn(DMHP)$_2$Cl·0.5H$_2$O were collected on a Nonius Kappa CCD diffractometer. The selected crystallographic data are listed in Table 1. Crystals were mounted on a glass fiber in a random orientation. Preliminary examination and data collection were performed using graphite monochromated Mo Kα radiation ($\lambda = 0.71073$ Å). Cell constants and an orientation matrix for data collection were obtained from least-squares refinement, using the setting angles in the range of $0 < \theta < 20°$ for both Mn(DMHP)$_3$·12H$_2$O and Mn(DMHP)$_2$Cl·0.5H$_2$O. For the complex Mn(DMHP)$_3$·12H$_2$O, a total of 4502 reflections were collected and 2189 reflections were unique. For the complex Mn(DHP)$_2$Cl·0.5H$_2$O, a total of 5306 reflections were collected and 3346 reflections were unique. Lorentz and polarization corrections were applied to the data. A linear absorption coefficient is 9.2/cm for Mo Kα radiation. An empirical correction was applied using the program SCALEPACK.[35] The structure was solved using the structure solution program PATTY in DIRDIF99[36] and was refined on a AlphaServer 2100 using SHELXL97.[37] Crystallographic drawings were produced using the program ORTEP.

Table 1. Selected Crystallographic Data of Mn(DMHP)$_3$·12H$_2$O and Mn(DMHP)$_2$Cl·0.5H$_2$O

formula	$C_{21}H_{48}MnN_3O_{18}$	$C_{14}H_{17}ClMnN_2O_{4.5}$
fw	685.56	375.69
space group	P3 (No. 147)	$P2_{1/c}$ (No. 14)
a, Å	16.5838 (18)	14.5962 (17)
b, Å	16.5838 (18)	13.3545 (19)
c, Å	6.8081 (18)	15.8059 (15)
α, degree	90.00	90.00
β, degree	90.00	102.282 (7)
γ, degree	120.00	90.00
V, Å^3	1621.5 (5)	3010.5 (6)
Z	2	8
d_{calc}, g/cm^3	1.404	1.658
T, K	150	150
cryst dimensions, mm^3	0.35 × 0.33 × 0.30	0.35 × 0.30 × 0.10
radiation (λ, Å)	Mo Kα (0.71073)	Mo Kα (0.71073)
linear absorption coefficient, mm^{-1}	0.464	1.043
transm factors	0.70−0.87	0.61, 0.90
$R(F_0)$	0.052[a]	0.063[a]
$R_w(F_0^2)$	0.106[b]	0.113[b]

[a] $R = \sum||F_0| - |F_c||/\sum|F_0|$ for $F_0^2 > 2\sigma(F_0^2)$. [b] $R_w = [\sum w(|F_0^2| - |F_c^2|)^2/\sum w|F_0^2|^2]^{1/2}$.

Results

Synthesis. We prepared the complex Mn(DMHP)$_2$Cl by reacting Mn(II) chloride with 2 equiv of DMHP under reflux in the presence of triethylamine. Recrystallization from a mixture of acetonitrile and ethanol (v:v = 1:1) afforded crystals suitable for X-ray crystallographic analysis. Mn(DMHP)$_3$ was prepared from the reaction of Mn(II) acetate with 3 equiv of DMHP in the presence of sodium acetate. It could also be prepared by reacting $Mn(OAc)_3$·2H$_2$O with 3 equiv of DMHP in the presence of triethylamine. Mn(DMHP)$_3$ is soluble in methanol and water. Recrystallization from water produced dark-green crystals suitable for X-ray crystallographic analysis.

Characterization. Mn(DMHP)$_2$Cl and Mn(DMHP)$_3$ were characterized by elemental analysis, IR, and ESI-MS methods. The IR spectra of these complexes show a strong and broad band at ~3450 cm^{-1} due to crystallization water molecules and four strong bands at a frequency of 1600−1400 cm^{-1}, which are characteristic for the coordinated 3,4-HPs. These four bands have been collectively assigned to $\upsilon_{C=O}$ and υ_{ring} since resolving these two different modes is extremely difficult because of mixing. The UV−vis absorption spectra (Figure 1S) of Mn(DMHP)$_2$Cl and Mn(DMHP)$_3$ in acetonitrile exhibit two sets of peaks in the 280−310- and 400−700-nm regions. Both Mn(DMHP)$_2$Cl and Mn(DMHP)$_3$ do not exhibit EPR signals at the perpendicular mode at 120 K. The ES-MS spectral and elemental analysis data are consistent with their proposed formula and have been

(35) Otwinowski, Z.; Minor, W. *Methods Enzymol.* **1997**, *276*, 307.
(36) Beurskens, P. T.; Beurskens, G.; deGelder, R.; Garcia-Granda, S.; Gould, R. O.; Israel, R.; Smits, M. M. *The DIRDIF-99 Program System. Crystallography Laboratory*; University of Nijmegen: The Netherlands, 1999.
(37) Shelderick, G. M. *SHELXL 97. A Program for Crystal Structure Refinement*; University of Göttingen: Göttingen, Germany, 1997.

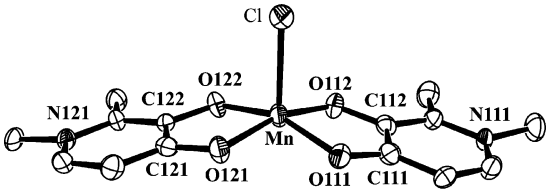

Figure 2. ORTEP drawing of $Mn(DMHP)_2Cl$ (ellipoids are at 50% probability). Crystallization water and hydrogen atoms are omitted for the sake of clarity.

Table 2. Selected Bond Distances of $Mn(DMHP)_3 \cdot 12H_2O$ and $Mn(DMHP)_2Cl \cdot 0.5H_2O$

$Mn(DMHP)_3 \cdot 12H_2O$			$Mn(DMHP)_2Cl \cdot 0.5H_2O$		
atom 1	atom 2	distance (Å)	atom 1	atom 2	distance (Å)
Mn	O(2)	1.9949 (18)	Mn(1)	O(112)	1.884 (4)
Mn	O(2)	1.9949 (18)	Mn(1)	O(111)	1.907 (4)
Mn	O(2)	1.9949 (18)	Mn(1)	O(121)	1.919 (4)
Mn	O(1)	2.028 (2)	Mn(1)	O(122)	1.922 (4)
Mn	O(1)	2.028 (2)	Mn(1)	Cl(1)	2.4149 (17)
Mn	O(1)	2.028 (2)			

confirmed by X-ray crystallographic analysis of $Mn(DMHP)_3 \cdot 12H_2O$ and $Mn(DMHP)_2Cl \cdot 0.5H_2O$.

X-ray Crystal Structure of $Mn(DMHP)_2Cl \cdot 0.5H_2O$. Figure 2 shows the ORTEP view of $Mn(DMHP)_2Cl \cdot 0.5H_2O$. Crystallization water and hydrogen atoms are omitted for the sake of clarity. Selected crystallographic data are listed in Table 1. There are eight $Mn(DMHP)_2Cl$ molecules in each unit cell, along with each crystallization water molecule forming hydrogen bond with two pyridinonato-oxygen atoms of two neighboring $Mn(DMHP)_2Cl$ molecules. The Mn atom is coordinated by two bidentate DMHP ligands and a chloride anion to form the neutral Mn(III) complex. The coordination geometry is best described as distorted square pyramid with four oxygen donors occupying the square plane and the chlorine atom occupying the apical site. The two DMHP ligands are in the cis position with two methyl groups on the same side. The coordination geometry of $Mn(DMHP)_2Cl$ is between those of Mn(salen)Cl (salen = N,N′-ethylenebis(salicylaldimine))[38] and Mn(L)Cl (L = N,N′-ethylenebis(3-formyl-5-methylsalicylaldimine)).[39] The Mn atom in $Mn(DMHP)_2Cl$ is ~0.25 Å above the square plane defined by four oxygen donor atoms, while Mn is 0.19 Å above the square plane defined by N_2O_2 donors in Mn(salen)Cl and 0.3035 Å above the square plane defined by the N_2O_2 donors in Mn(L)Cl (L = N,N′-ethylenebis(3-formyl-5-methylsalicylaldimine)).

The average Mn−O (carbonyl) bond length is 1.903 (4) Å (Table 2). Surprisingly, the average Mn−O (hydroxy) bond distance is 1.913 (4) Å, which is ~0.01 Å longer than that of the Mn−O (carbonyl) bond. Compared to that of the free ligand, the C=O bond is longer by 0.036 Å, while the C−O bond is ~0.01 Å shorter in the complex $Mn(DMHP)_2Cl$. The average Mn−O bond distances are ~0.10 Å shorter than those observed in $Mn(DMHP)_3 \cdot 12H_2O$, most likely due to their differences in the coordination number. The Mn−Cl bond distance is 2.4149 (17) Å, which is compared well to those found in complexes Mn(salen)Cl (Mn−Cl = 2.461(1) Å)[38] and Mn(L)Cl (Mn−Cl = 2.3691(14) Å, L = N,N′-ethylenebis(3-formyl-5-methylsalicylaldimine)).[39]

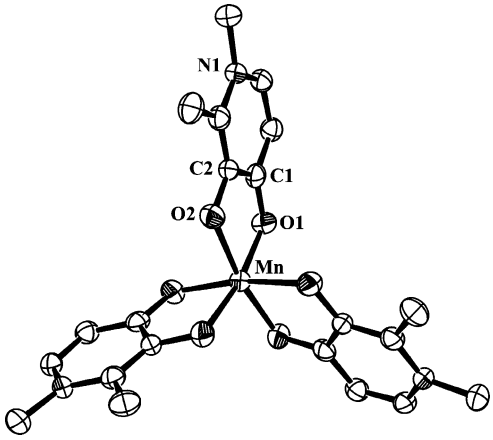

Figure 3. ORTEP drawing of $Mn(DMHP)_3$ (ellipoids are at 50% probability). Crystallization water and hydrogen atoms are omitted for the sake of clarity.

X-ray Crystal Structure of $Mn(DMHP)_3 \cdot 12H_2O$. Figure 3 shows the ORTEP view of $Mn(DMHP)_3 \cdot 12H_2O$. Crystallization waters and hydrogen atoms are omitted for the sake of clarity. Figure 4 shows a unit cell packing diagram of the complex $Mn(DMHP)_3 \cdot 12H_2O$ (ellipoids are at 50% probability). Selected crystallographic data are listed in Table 1. The Mn atom is coordinated by three bidentate DMHP ligands. The coordination geometry is a distorted octahedron with a 3-fold symmetry along the *c* axis and is isostructural with complexes $M(DMHP)_3 \cdot 12H_2O$ (M = Al, Ga, Fe, and In).[27−30,33] Three-coordinated DMHP ligands are in the facial configuration, which is typical of tris-DMHP exoclathrate metal complexes. Each $Mn(DMHP)_3$ molecule is crystallized with 12 water molecules in an extensive hydrogen-bonding network between crystallization water molecules (formed in bridges and cylinders) and the coordinated pyridinonato-oxygen atoms. The hydrogen-bonding interactions in the water cylinders in $M(DMHP)_3 \cdot 12H_2O$ (M = Al, Ga, and In) have been described in details by Orvig and co-workers.[27−30]

The Mn−O1 bond length is 2.028 (2) Å and the Mn−O2 bond distance is 1.995 (5) Å (Table 2). Upon metal chelation the negative charge of the deprotonated hydroxo-oxygen is delocalized through resonance extending from O1 to O2 through the C1−C2 bond. The carbonyl-oxygen atom withdraws more electron density when bonding to the metal ion with higher positive charge density. As a result, there is a shortening of C2−O2 and lengthening of the C1−O1 bond. Figure 5 shows the changes of selected bond distances from DMHP (in parentheses) to its Mn(III), Ga(III), and Fe(III) complexes. As expected, the C=O bond becomes longer than that in the free ligand by 0.021, 0.026, and 0.021 Å in its Mn(III), Ga(III), and Fe(III) complexes, respectively. The metal chelation brings about a shortening of the C−O (hydroxy) bond by 0.016, 0.021, and 0.021 Å in its Mn(III), Ga(III),[28] and Fe(III)[33] complexes. Similar results were also observed in $M(DMHP)_3 \cdot 12H_2O$ (M = Al and In).[27,28,30]

(38) Pecoraro, V. L.; Butler, W. M. *Acta Crystallogr.* **1986**, *C42*, 1151.
(39) Das, D.; Cheng, C. P. *J. Chem. Soc., Dalton Trans.* **2000**, 1081.

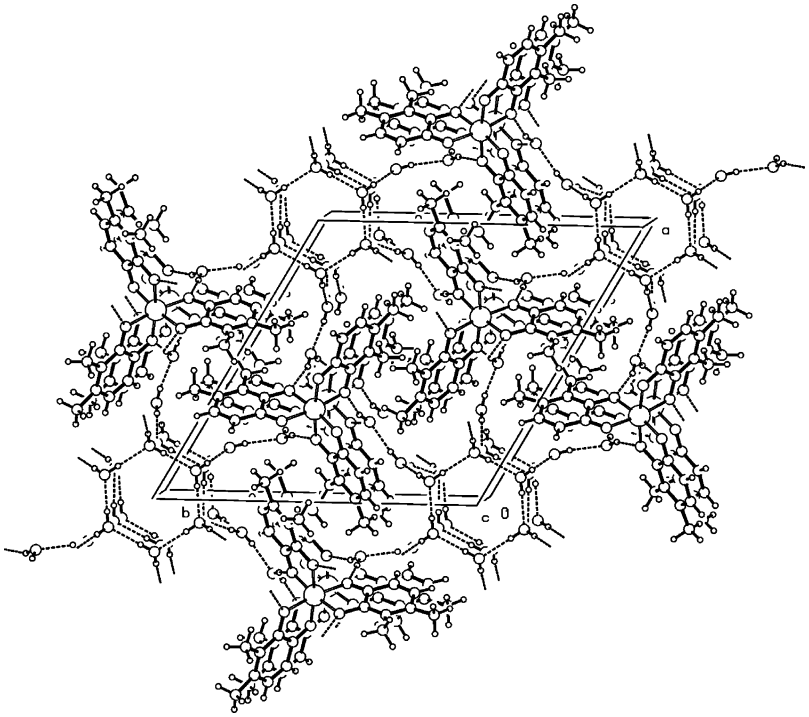

Figure 4. Unit cell packing diagram of the complex Mn(DMHP)$_3$·12H$_2$O (ellipoids are at 50% probability).

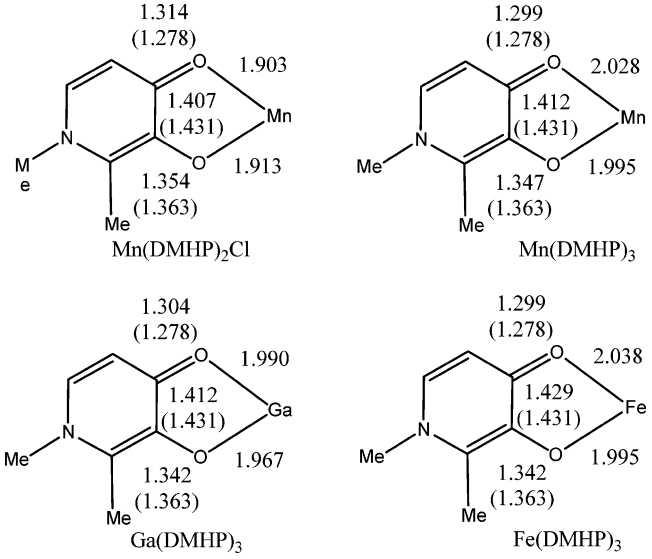

Figure 5. Comparison of bond distances in DMHP (in parentheses) and its Ga(III), Mn(III), and Fe(III) complexes.

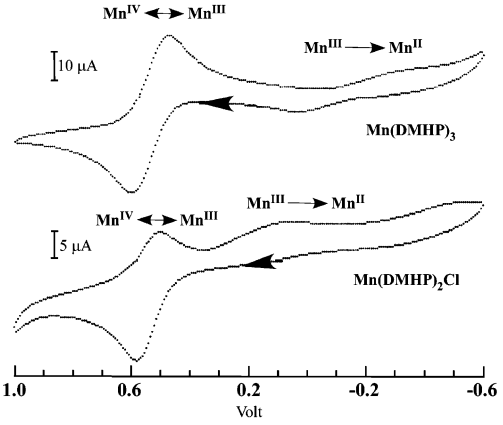

Figure 6. Cyclic voltammograms of Mn(DMHP)$_3$ (top) and Mn(DMHP)$_2$Cl (bottom). The concentrations of Mn(III) complexes were about 2 mM in acetonitrile. Potentials are given as those vs NHE since the Ag/AgCl electrode has a potential of +0.2 V vs NHE. The scan rate was 50 mV/s for both Mn(DMHP)$_3$ and Mn(DMHP)$_2$Cl.

Obviously the fact that the π delocalization is enhanced by metal chelation and the impact of Mn(III) is almost identical to that of Fe(III).

Electrochemistry. Cyclic voltammograms of Mn(DMHP)$_2$Cl and Mn(DMHP)$_3$ were recorded in acetonitrile with 0.1 M tetrabutylammonium hexafluorophosphate as the supporting electrolyte in the potential range from −0.8 to +0.8 V using a glassy-carbon working electrode, a Pt wire auxiliary electrode, and an Ag/AgCl in 3 M NaCl solution as the reference electrode. Figure 6 shows representative cyclic voltammograms of Mn(DMHP)$_2$Cl and Mn(DMHP)$_3$. Potentials are given as those vs NHE since the Ag/AgCl electrode has a potential of +0.2 V vs NHE. The initial cathodic scan shows an irreversible one-electron reduction wave at +0.05 V for Mn(DMHP)$_2$Cl and −0.2 V for Mn(DMHP)$_3$. These potentials were corresponding to the reduction of Mn(III) to Mn(II). Both Mn(DMHP)$_2$Cl and Mn(DMHP)$_3$ also show quasi-irreversible redox waves at +0.54 V, which corresponded to the Mn(III)/Mn(IV) couple. Room-temperature control potential oxidation experiments were performed on both Mn(III) complexes. During the oxidation, the solution color turned from green-brown to purple. The EPR spectrum (Figure 2S) of the electrochemically oxidized Mn frozen solution shows a broad signal at $g = 4.5$ and a weak six-line signal at $g = 2$.

Discussion

For the last two decades, a large number of HPs have been studied for their coordination chemistry with Fe(III),[33] Al-

(III),[27,28] Ga(III),[28] In(III),[30] Zn(II),[40,41] and Sn(II).[40] Recently, HPs have been proposed as matrix metalloproteinase (MMP) inhibitors for the treatment of cancer and other diseases.[42] Metal complexes of 3,4-HPs have been studied as metallopharmaceuticals. For example, neutral vanadyl(IV) complexes of hydroxypyrones and HPs have shown promising results as orally active insulin-enhancing agents.[43−46] Zn(II) and Tin(II) complexes of HPs are useful in dental care formulations,[41] while their ^{67}Ga, ^{111}In, and ^{99m}Tc complexes have been proposed as radiopharmaceuticals for scintigraphic imaging.[47−49] However, there is very little information available about their Mn(II) and Mn(III) complexes. We are interested in DMHP and related 3,4-HPs for their potential as Mn chelators for the treatment of chronic Mn toxicity.

Why Mn(III) Chelators? In a normal individual, the Mn level is under tight control by proteins such as tranferrin. However, Mn overload may become significant among workers in the mining, welding, and battery manufacturing industries. The Mn-induced neurodegenerative toxicity has been associated with a distorted iron metabolism at systemic and cellular levels.[15−17] It has been reported that following Mn exposure there is a predominant influx of Fe from blood into the CSF and from the extracellular matrix to intracellular space.[16,17] As a result, Fe also becomes overloaded intracellularly.[20] Since Fe(II) and Fe(III) are involved in the Fenton reaction, excess Fe often results in overproduction of hydroxyl or peroxide free radicals and leads to oxidative stress and diseases related to inflammation. Thus, an ideal Mn chelator should be able to remove excess Mn and Fe simultaneously from the intracellular matrix.

In the design of Mn chelators for clinical application, the metal selectivity and high stability of the resulting metal complex are prerequisite. In theory, chelators can be designed for either Mn(II) or Mn(III). Similar to Fe(III), the high-spin Mn(III) is a trivalent cation with the ionic radii of 0.645 Å and as such is classified as a hard Lewis acid by virtue of its high charge density. It forms stable Mn(III) complexes with hard donor atoms, such as oxygen donors of DFO and DMHP (Figure 1). In contrast, the Mn(II) cation has a lower charge density and prefers relatively softer donors such as the pyridine nitrogen.[22,23] Chelators with a high affinity for Mn(II) often form highly stable metal complexes of some biologically important metal ions, such as Cu(II) and Zn(II). Therefore, design of Mn(II)-selective chelators is an extremely difficult task. In contrast, Mn(III)-selective chelators are readily designed by using oxygen donors from hydroxamates, catechols, and HPs. Their coordination chemistry with Fe(III), Al(III), Ga(III), and In(III) has been studied extensively for the last two decades.[22−34] Another advantage of Mn(III)-selective chelators is that they are able to form a reasonably stable Mn(II) complex, which can be rapidly oxidized to form the corresponding Mn(III) complex. Thus, the Mn(III) chelators should be able to remove both Mn(II) and Mn(III) under physiological conditions.

Why 3,4-HPs? There are many Fe(III)-selective chelators useful for Mn-chelation therapy. These include DFO, EDTA analogues, hydroxamates, catechols, hydroxypyrones, and HPs. Among them, HPs are of particular interest. HPs combine the characteristics of hydroxamate and catechol groups, and form five-membered chelate rings in which the metal is bonded by two vicinal oxygen donors. HPs are monoprotic acids under physiological conditions (pH $\approx$ 7.0) and form highly stable tris-ligand Fe(III) complexes. Among different HPs, 3,4-HPs show the highest affinity and selectivity for Fe(III) due to delocalization of electrons in the pyridinone ring. HPs show high selectivity for trivalent metal ions over divalent metal ions, have small molecular weights (FW < 400 Dalton), and are able to crossing the blood−brain barrier.[50] All these factors make 3,4-HPs ideal chelators for the removal of excess intracellular Mn and Fe. DMHP is our first choice because it has been approved for the treatment of iron overload in β-thalassemia patients.[22−26]

Mn(DMHP)$_2$Cl. Since chloride ions are abundant in the blood circulation, one can envision that DMHP may form both bis-ligand and tris-ligand complexes when bonding to Mn(III) in the biological system. We prepared Mn(DMHP)$_2$Cl in order to compare its structural and redox properties with those of Mn(DMHP)$_3$. In the solid state, Mn(III) is five-coordinated with the O_4Cl donor atoms arranged in a distorted square pyramidal geometry (Figure 2), with Cl in the axial position. This represents a rare example of five-coordinated Mn(III) complexes with two bidentate ligands and a distorted square pyramidal geometry. However, the most unusual feature of Mn(DMHP)$_2$Cl is that the average Mn−O (hydroxy) bond distance is ~0.01 Å longer than that of the Mn−O (carbonyl) bonds. In complexes M(DMHP)$_3$ (M = Al, Fe, Ga, In, and Mn), the M−O (hydroxyl) bond distances are always shorter than those of M−O (carbonyl) due to the negative charge of the deprotonated hydroxyl group. A shorter Mn−O (carbonyl) bond in Mn(DMHP)$_2$Cl strongly suggests that there is more extensive delocalization of electrons between carbonyl and hydroxyl groups, which makes the pyridinone ring more close to the catechol-type of aromatic systems.

Mn(DMHP)$_3$. Mn(DMHP)$_3$ was prepared from the reaction of Mn(II) or Mn(III) with 3 equiv of DMHP. The X-ray crystallographic analysis shows that the Mn(III) is coordinated by three DMHP ligands with six oxygen donor atoms

(40) Ahmed, S. I.; Burgess, J.; Fawcett, J.; Parsons, S. A.; Russell, D. R.; Laurie, S. H. *Polyhedron* **2000**, *19*, 129.
(41) Barret, M. C.; Mahon, M. F.; Molloy, K. C.; Steed, J. W.; Wright, P. *Inorg. Chem.* **2001**, *40*, 4384.
(42) Puerta, D. T.; Cohen, S. M. *Inorg. Chem.* **2003**, *42*, 3423.
(43) McNeill, J. H.; Yuen, V. G.; Hoveyda, H. R.; Orvig, C. *J. Med. Chem.* **1992**, *35*, 1489.
(44) Caravan, P.; Gelmini, L.; Glover, N.; Herring, F. G.; Li, H.; McNeill, J. H.; Rettig, S. J.; Styawati, I. A.; Shuter, E.; Sun, Y.; Tracey, A. S.; Yuen, V. G.; Orvig, C. *J. Am. Chem. Soc.* **1995**, *117*, 12759.
(45) Thompson, K. H.; Orvig, C. *Coord. Chem. Rev.* **2001**, *219*, 1033 and references therein.
(46) Thompson, K. H.; Orvig, C. *J. Chem. Soc., Dalton Trans.* **2000**, 2885 and references therein.
(47) Zhang, Z. H.; Lyster, D. M.; Webb, G. A.; Orvig, C. *Nucl. Med. Biol.* **1992**, *19*, 327.
(48) Edwards, D. S.; Liu, S.; Lyster, D. M.; Poirier, M. J.; Vo, C.; Webb, G. A.; Zhang, Z. H.; Orvig, C. *Nucl. Med. Biol.* **1993**, *20*, 857.
(49) Edwards, D. S.; Liu, S.; Poirier, M. J.; Zhang, Z. H.; Webb, G. A.; Orvig, C. *Inorg. Chem.* **1994**, *33*, 5607.
(50) Habgood, M. D.; Liu, Z. D.; Dehkordi, L. S.; Khodr, H. H.; Abott, J.; Hider, R. C. *Biochem. Pharmacol.* **1999**, *57*, 1305.

Table 3. Selected Bond Angles of Mn(DMHP)$_3$·12H$_2$O and Mn(DMHP)$_2$Cl·0.5H$_2$O

Mn(DMHP)$_3$·12 H$_2$O				Mn(DMHP)$_2$Cl·0.5 H$_2$O			
atom 1	atom 2	atom 3	angle (deg)	atom 1	atom 2	atom 3	angle (deg)
O(2)	Mn	O(2)	91.58(8)	O(112)	Mn(1)	O(111)	85.49 (16)
O(2)	Mn	O(2)	91.58(8)	O(112)	Mn(1)	O(121)	163.26 (17)
O(2)	Mn	O(2)	91.58(8)	O(111)	Mn(1)	O(121)	89.21(16)
O(2)	Mn	O(1)	96.00(8)	O(112)	Mn(1)	O(122)	93.92 (16)
O(2)	Mn	O(1)	81.77(8)	O(111)	Mn(1)	O(122)	158.69 (17)
O(2)	Mn	O(1)	170.03(8)	O(121)	Mn(1)	O(122)	85.29 (16)
O(2)	Mn	O(1)	170.03(8)	O(112)	Mn(1)	Cl(1)	99.55 (13)
O(2)	Mn	O(1)	96.00(8)	O(111)	Mn(1)	Cl(1)	101.52(12)
O(2)	Mn	O(1)	81.77(8)	O(121)	Mn(1)	Cl(1)	97.06(13)
O(2)	Mn	O(1)	91.49(8)	O(122)	Mn(1)	Cl(1)	99.58(12)
O(1)	Mn	O(1)	81.77(8)				
O(2)	Mn	O(1)	170.03(8)				
O(2)	Mn	O(1)	96.00(8)				
O(1)	Mn	O(1)	91.49(8)				
O(1)	Mn	O(1)	91.49(8)				
C(1)	O(1)	Mn	111.51(17)				
C(2)	O(2)	Mn	111.28(16)				

in a facial or distorted octahedral configuration (Figure 3), which is typical for exoclathrate metal complexes M(DMHP)$_3$·12H$_2$O (M = Al, Ga, Fe, and In).[27−30,33] High-spin Mn(III) complexes with octahedral geometry often show a Jahn−Teller distortion, either elongation or contraction, due to its electron d^4 configuration.[51] The difference between "long" and "short" Mn−X (X = O, N, S, Cl) bond distance in the Jahn−Teller distortion is generally greater than 0.1 Å. The fact that all three Mn−O (carbonyl) and Mn−O (hydroxyl) bond distances in Mn(DMHP)$_3$ are identical clearly demonstrates that there is no Jahn−Teller distortion. This represents a rare example of octahedral Mn(III) complexes without Jahn−Teller distortion. Hartman and co-workers reported the structure of the tris(catecholate)Mn(IV) complex, [Mn(3,5-(*t*-Bu)$_2$Cat)$_3$]$^{2-}$,[52] in which Mn(IV) was highly stabilized due to the short "bite distance" of catechol (2.58 Å). However, there is no structure reported for the tris(semiquinone)Mn-(III) complex. The "bite distance" of DMHP is 2.63 Å, which is slightly longer than that of catecholate (2.58 Å) but not enough for Mn(DHMP)$_3$ to accommodate Jahn−Teller distortion.

The structure of Mn(DMHP)$_3$·12H$_2$O is almost identical to that of Fe(DMHP)$_3$·12H$_2$O due to the similarity between Mn(III) and Fe(III) with respect to their ionic radii and charge density. The charge density is related to the size of the metal ion, the strength of the M−O bonds, the degree of delocalization of the O1−C1−C2−O2 bonding system, and the decrease of the C1−C2 bond length. Table 4 lists selected bond lengths and angles for the oxygen donor atoms to the trivalent metal ions. Obviously, the M−O (hydroxy) bond is shorter than the M−O (carbonyl) due to the negative charge of the hydroxy O atom. The M−O bond distances show a regular trend of In(III) ≫ Fe(III) ≈ Mn(III) > Ga-(III) ≫ Al(III). In some way, the M−O bond distances can be used to estimate the stability of tris-DMHP metal complexes. For example, the Ga−O (hydroxy) bond is ∼0.03 Å shorter than that of Fe−O (hydroxy) and Ga(DMHP)$_3$ (log β_3 = 38.42)[32] has a higher stability than that of Fe(DMHP)$_3$ (log β_3 = 35.9).[53,54] In(DMHP)$_3$ (log β_3 = 32.93)[32] is less stable than Ga(DMHP)$_3$ and Fe(DMHP)$_3$ due to the longer In−O bond distances (by almost 0.14 Å). Since the Mn−O bond distances in Mn(DMHP)$_3$ are almost identical to those of Fe−O bonds, Mn(DMHP)$_3$ should have the stability close to that of Fe(DMHP)$_3$. However, this estimation ignores the impact of their electronic configurations on the stability of metal complexes. Studies to determine the stability constants of Mn(III) complexes of DMHP and related analogues are still in progress.

Table 4. Average Bond Distances and Bond Angles in Tris-Ligand Complexes M(DMHP)$_3$·12H$_2$O (M = Al, Ga, Fe, In, and Mn)

metal ion	Al(III)	Ga(III)	Fe(III)	Mn(III)	In(III)
ionic radii (Å)	0.535	0.620	0.645	0.645	0.800
M−O (C=O) (Å)	1.923(2)	1.990(3)	2.046(3)	2.028 (2)	2.165 (2)
M−O (C−OH) (Å)	1.893(2)	1.967(3)	1.998(3)	1.995 (2)	2.134 (2)
Δ(M−O) (Å)	0.030(2)	0.023(3)	0.048(3)	0.033 (2)	0.031 (2)
C−O (C−OH) (Å)	1.327(3)	1.342(5)	1.346(4)	1.347(4)	1.343(3)
C−O (C=O) (Å)	1.299(3)	1.304(5)	1.287(4)	1.299(3)	1.289(3)
C1−C2 (Å)	1.423(3)	1.409(6)	1.410(5)	1.412(4)	1.403(3)
O−M−O (cis) (deg)	84.23(6)	83.22(6)	80.8(1)	81.77(8)	77.87(6)

UV−Vis Spectroscopy. The absorption spectra for Mn-(DMHP)$_2$Cl and Mn(DMHP)$_3$ display an intense ligand-to-metal charge-transfer transition (LMCT) in the 280−310 nm region (ϵ = 10 000−26 000 M^{-1} cm^{-1}), from the hydroxyl O to Mn(III) LMCT. The weaker transitions (ϵ = 200−500 M^{-1} cm^{-1}) in the 400−700-nm region are due to d−d transitions. The absorption spectrum of Mn(DMHP)$_2$Cl is compared well with those of tris(Schiff-base) Mn(III) complexes with Jahn−Teller distortion.[55]

Electrochemistry. Mn(DMHP)$_2$Cl and Mn(DMHP)$_3$ show irreversible reduction waves for Mn(III) to Mn(II) at +0.05 V and −0.2 V, respectively, vs NHE. The low reduction potential for the Mn(III)/Mn(II) couple suggests that the Mn-(III) oxidation state is highly stabilized and the irreversibility suggests that reduction from Mn(III) to Mn(II) probably involves dissociation of the DMHP ligand for Mn(DMHP)$_3$ or chloride coligand for Mn(DMHP)$_2$Cl, and requires a significant conformational change. The reduction potential of Mn(DMHP)$_2$Cl and Mn(DMHP)$_3$ is compared well with that of tris(quinolin-8-olato)manganese(III) (−0.16 V).[56,57] Other known reduction potentials for Mn(III) complexes include tris(pyridino-2-carboxylato)manganese(III) (+0.62 V),[56,57] Mn(tcta) (tcta = 1,4,7-triazacyclononane-N,N′,N″-triacetate) (+0.80 V),[58] Mn(tacn) (tacn = 1,4,7-tris(*tert*-butyl-2-hydroxybenzyl)-1,4,7-triazacyclononane) (−0.58 V),[59] and Mn(III) complexes of hexadentate N_4O_2 and N_3O_3 Schiff-

(51) Stults, B. R.; Marianelli, R. S.; Day, V. W. *Inorg. Chem.* **1979**, *18*, 1853 and references therein.
(52) Hartman, J. R.; Foxman, B. M.; Cooper, S. R. *Inorg. Chem.* **1984**, *23*, 1381.
(53) Clarke, E. T.; Martell, A. E. *Inorg. Chim. Acta* **1992**, *191*, 57.
(54) Moetekaitis, R. J.; Martell, A. E. *Inorg. Chim. Acta* **1991**, *183*, 71.
(55) Ramesh, K.; Bhuniya, D.; Mukherjee, R. *J. Chem. Soc., Dalton Trans.* **1991**, 2917.
(56) Yamaguchi, K.; Sawyer, D. T. *Inorg. Chem.* **1985**, *24*, 971.
(57) Richert, S. A.; Tsang, P. K. S.; Sawyer, D. T. *Inorg. Chem.* **1989**, *28*, 2471.
(58) Wiegardt, K.; Bossek, U.; Chaudhuri, P.; Herrmann, W.; Menke, B. C.; Weiss, J. *Inorg. Chem.* **1982**, *21*, 4308.
(59) Auerbach, U.; Eckert, U.; Wiegardt, K.; Nuber, B.; Weiss, J. *Inorg. Chem.* **1990**, *29*, 938.

base ligands.[55,60,61] $Mn(DMHP)_2Cl$ and $Mn(DMHP)_3$ also showed a quasi-reversible oxidation wave at +0.54 V from Mn(III) to Mn(IV). These potentials are compared well to those of Mn(III)/Mn(IV) complexes of hexadentate N_4O_2 and N_3O_3 and Schiff-base ligands.[55,60,61] However, they are much lower than that of tris(quinolin-8-olato)manganese(III) (+1.18 V).[56,57] Other known oxidation potentials for mononuclear Mn(III) complexes also include tris(pyridino-2-carboxylato)-manganese(III) (+1.61 V)[55,56] and Mn(tacn) (tacn = 1,4,7-tris(*tert*-butyl-2-hydroxybenzyl)-1,4,7-triazacyclononane) (−0.05 V).[58] The difference in oxidation potentials of these Mn(III) complexes reflects the nature of donor atoms in the chelators. The high oxidation potential for $Mn(DMHP)_2Cl$ and $Mn(DMHP)_3$ suggests that the Mn(III) is highly favored over Mn(IV). By the controlled potential oxidation, both $Mn(DMHP)_2Cl$ and $Mn(DMHP)_3$ can be oxidized to produce the corresponding Mn(IV) complexes, the perpendicular-mode EPR spectra of which show a typical broad signal centered at $g = 4.2$ and a weak 6-line signal centered at $g = 2$ for Mn(IV) with the $^4A_{3/2}$ ground state (Figure 2S). The EPR data clearly demonstrated that the quasi-reversible oxidation waves at +0.54 V for $Mn(DMHP)_3$ and $Mn(DMHP)_2Cl$ are indeed from Mn(III) to Mn(IV).

Conclusions

To understand the coordination chemistry of Mn(III) with DMHP and HPs, we have prepared two Mn(III) complexes, $Mn(DMHP)_3$, and $Mn(DMHP)_2Cl$, which have been characterized by elemental analysis, IR, EPR, ESI-MS, and X-ray crystallography. The X-ray crystal structure of $Mn(DMHP)_2Cl\cdot 0.5H_2O$ revealed a rare example of five-coordinated Mn(III) complexes with two bidentate ligands and the square pyramidal coordination geometry. Surprisingly, the average Mn−O (hydroxy) bond distance is ∼0.025 Å longer than that of the Mn−O (carbonyl) bond in $Mn(DMHP)_2Cl\cdot 0.5H_2O$, suggesting an extensive delocalization of electrons in the pyridinone rings. In the solid state, the complex $Mn(DMHP)_3\cdot 12H_2O$ is isostructural to complexes $M(DMHP)_3\cdot 12H_2O$ (M = Al, Ga, Fe, and In) and has no Jahn−Teller distortion. The electrochemical data for $Mn(DMHP)_3$ and $Mn(DMHP)_2Cl$ suggests that the Mn(III) oxidation state is highly stabilized by three DMHP ligands. DMHP has the potential as a chelator for the removal of excess intracellular Mn and the treatment of chronic Mn toxicity.

Acknowledgment. Acknowledgment is made to Dr. Phillip E. Fanwick, Department of Chemistry, Purdue University, for X-ray crystallography of $Mn(DMHP)_2Cl\cdot 0.5H_2O$ and $Mn(DMHP)_3\cdot 12H_2O$. Authors also thank Professor Vincent L. Pecoraro and the Department of Chemistry, University of Michigan, for the use of their EPR spectrometer. This work is supported by Purdue University and Bristol-Myers Squibb Medical Imaging, Inc.

Supporting Information Available: X-ray crystallographic files are in CIF format for the reported structures of $Mn(DMHP)_2Cl\cdot 0.5H_2O$ and $Mn(DMHP)_3\cdot 12H_2O$, electronic absorption spectra of $Mn(DMHP)_3$ and $Mn(DMHP)_2Cl$, and a perpendicular EPR spectrum of oxidized $Mn(DMHP)_3$. These materials are available free of charge at http://pubs.acs.org.

IC0490627

(60) Panja, A.; Shaikh, N.; Gupta, S.; Butcher, R. J.; Banerjee, P. *Eur. J. Inorg. Chem.* **2003**, 1540.
(61) Neves, A.; Erthal, S. M. D.; Vencato, I.; Ceccato, A. S.; Mascarenhas, Y. P.; Nascinmento, O. R.; Hörner, M.; Batista, A. A. *Inorg. Chem.* **1992**, *31*, 4749.